Supplementary material for the article:

Rusmirović, J.D., Obradović, N., Perendija, J., Umićević, A., Kapidžić, A., Vlahović, B., Pavlović, V., Marinković, A.D., Pavlović, V.B., 2019. Controllable synthesis of Fe3O4-wollastonite adsorbents for efficient heavy metal ions/oxyanions removal. Environ Sci Pollut Res 26, 12379–12398. https://doi.org/10.1007/s11356-019-04625-0

Supplementary material

Controllable Synthesis of Fe_3O_4-Wollastonite Adsorbents for Efficient Heavy Metal Ions/Oxyanions Removal

Jelena D. Rusmirović[1*], Nina Obradović[2], Jovana Perendija[3], Ana Umićević[4], Ana Kapidžić[4], Branislav Vlahović[5], Vera Pavlović[6], Aleksandar D. Marinković[7], Vladimir B. Pavlović[2,8]

[1]Innovation Center of the Faculty of Technology and Metallurgy, University of Belgrade, Karnegijeva 4, 11120 Belgrade, Serbia, jrusmirovic@tmf.bg.ac.rs
[2]Institute of Technical Sciences of SASA, Knez Mihailova 35/IV, 11000 Belgrade, Serbia
[3]Institute of Chemistry, Technology and Metallurgy, University of Belgrade, Njegoševa 4, 11000, Serbia
[4]Vinča Institute of Nuclear Sciences, University of Belgrade, Serbia
[5]North Carolina Central University, Department of Mathematics and Physics, Durham, United States
[6]Faculty of Mechanical Engineering, Kraljice Marije 16, 11120 Belgrade, Serbia
[7]Faculty of Technology and Metallurgy, University of Belgrade, Karnegijeva 4, 11120 Belgrade, Serbia
[8]Faculty of Agriculture, University of Belgrade, Nemanjina 6, 11080 Belgrade-Zemun, Serbia

[*]***Corresponding author***: Jelena Rusmirović, Innovation Center of the Faculty of Technology and Metallurgy, University of Belgrade, Karnegijeva 4, 11120 Belgrade, Serbia, jrusmirovic@tmf.bg.ac.rs

Scanning electron microscopy (SEM)

Table S1. EDS mapping results of WL/MG and WL-γ-APS/MG adsorbents

WL/MG adsorbent						
Element	Line Type	Apparent Concentration	k Ratio	Wt%	Wt% Sigma	Standard Label
C	K series	1.51	0.01510	13.92	0.10	C Vit
O				55.13		
Si	K series	4.35	0.03449	8.34	0.03	SiO_2
Ca	K series	9.79	0.08749	18.24	0.05	Wollastonite
Fe	K series	1.93	0.01929	4.37	0.05	Fe
Total:				100.00		
WL-γ-APS/MG adsorbent						
Element	Line Type	Apparent Concentration	k Ratio	Wt%	Wt% Sigma	Standard Label
C	K series	1.94	0.01942	16.78	0.06	C Vit
O				57.44		
Si	K series	2.54	0.02011	5.04	0.02	SiO_2
Ca	K series	5.02	0.04489	9.38	0.02	Wollastonite
Fe	K series	5.02	0.05016	11.36	0.04	Fe
Total:				100.00		

Effect of pH on Cd^{2+} and Ni^{2+} ions removal by W-MG and W-γ-APS/MG

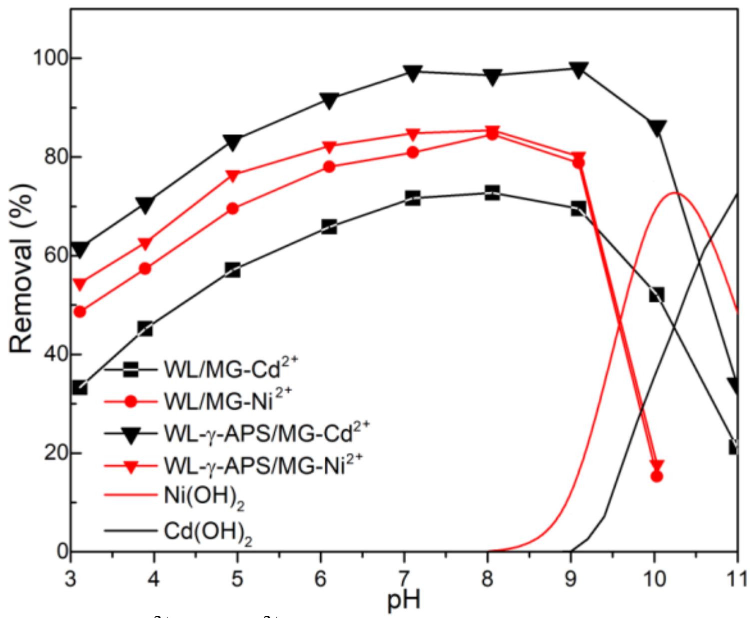

Figure S1. Influence of pH on Cd^{2+} and Ni^{2+} ions removal by W-MG and W-γ-APS/MG ($C_i[Cd^{2+}]=C_i[Ni^{2+}]=10\mu gl^{-1}$, m/V = 125mgl^{-1}, T = 308K)

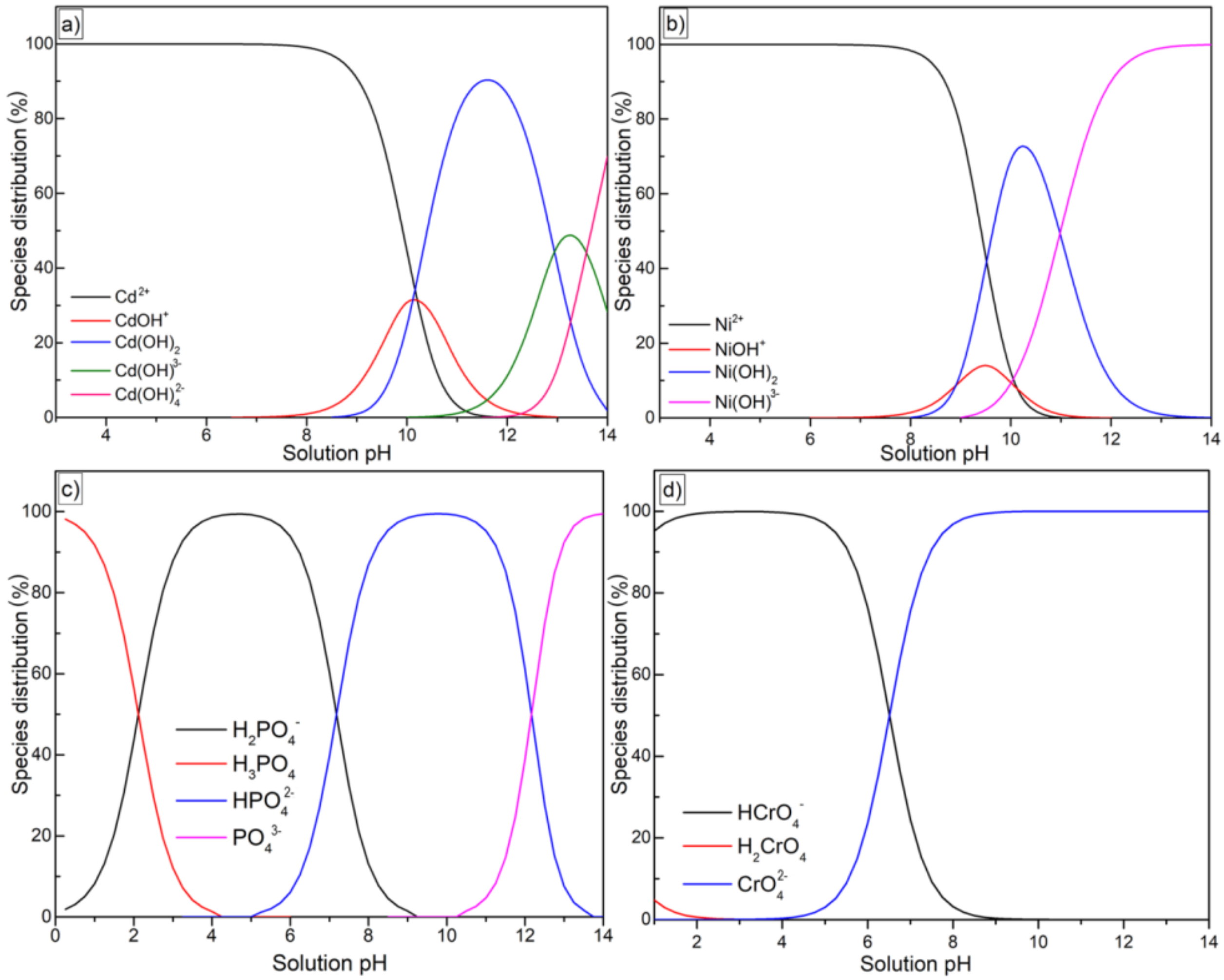

Figure S2. Speciation of: a) Cd^{2+}, b) Ni^{2+}, c) $H_2PO_4^-/HPO_4^{2-}$ and d) $HCrO_4^-/CrO_4^{2-}$ obtained using MINTEQ. 3.0 software (C = 25mg l^{-1}, T = 308K)

Adsorption/desorption study of Cd^{2+}, Ni^{2+}, $HCrO_4^-/CrO_4^{2-}$ and $H_2PO_4^-/HPO_4^{2-}$ on WL/MG and WL-γ-APS/MG adsorbents.

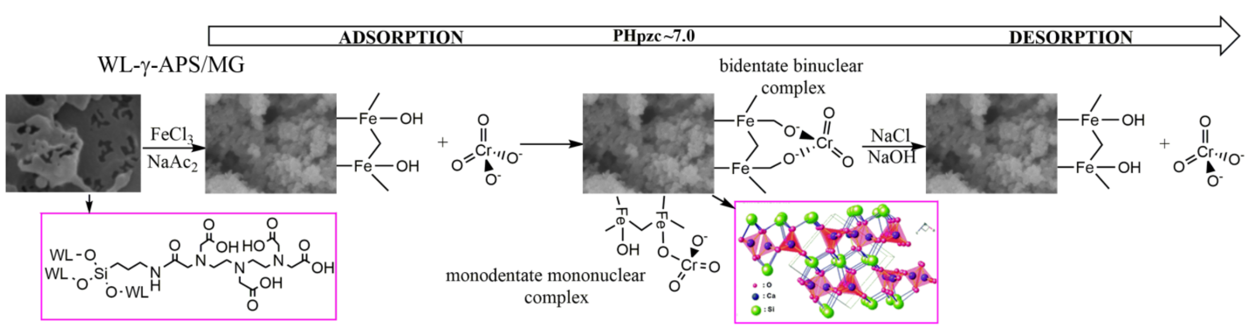

Figure S3. Schematic illustration of formation of monodentate and bidentate complexes between MG modified WL and $HCrO_4^-/CrO_4^{2-}$ ions

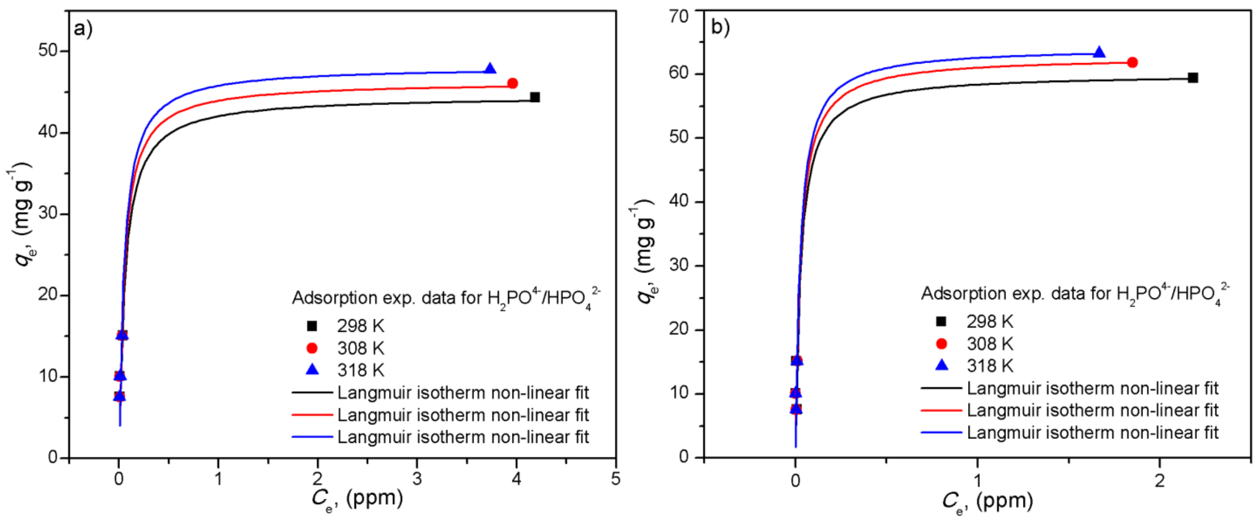

Figure S4. Non-linear Langmuir adsorption isotherms for $H_2PO_4^-/HPO_4^{2-}$ ions on a) WL-MG and b)WL-γ-APS/MG adsorbents at 298, 308 and 318K. Lines: non-linear Langmuir model ($m_{adsorrbent}$= 1.0, 1.5, 2.5, 5.0, 7.5 and 10 mg, C_i = 10 ppm, pH 6.5 for $H_2PO_4^-/HPO_4^{2-}$)

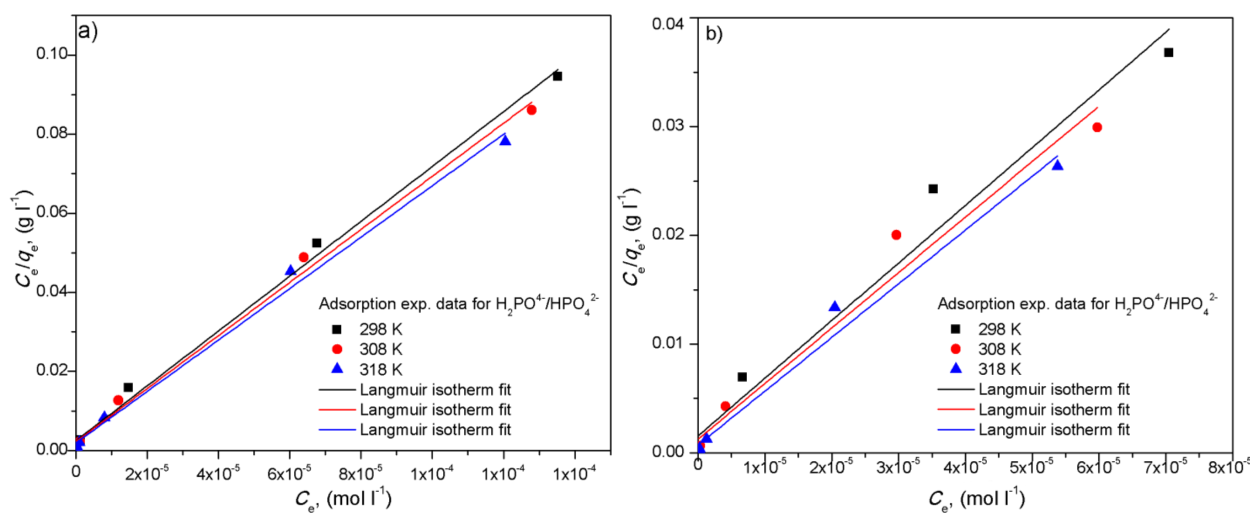

Figure S5. Linear Langmuir adsorption isotherms for $H_2PO_4^-/HPO_4^{2-}$ ions on a) WL-MG and b) WL-γ-APS/MG adsorbents at 298, 308 and 318K. Lines: Langmuir model ($m_{adsorrbent}$= 1.0, 1.5, 2.5, 5.0, 7.5 and 10 mg, C_i = 10 ppm, pH 6.5 for $H_2PO_4^-/HPO_4^{2-}$)

Table S2. Linear Langmuir isotherm parameters for Cd^{2+} and Ni^{2+}ions obtained at 298, 308 and 318 K using WL/MG and WL-γ-APS/MG adsorbents

	Cd^{2+}					Ni^{2+}				
	T **(K)**	q_e **(mg g^{-1})**	***K*** **(l mg^{-1})**	K_L **(l mol^{-1})**	R^2	q_e **(mg g^{-1})**	***K*** **(l mg^{-1})**	K_L **(l mol^{-1})**	R^2
WL/MG	298	51.015	26.676	83933651	0.997	48.538	26.404	83074307	0.992
	308	53.961	28.122	88487326	0.996	50.926	27.729	87248571	0.996
	318	55.749	29.555	92993521	0.995	52.406	29.516	92869758	0.998
WL-γ-APS/MG	298	69.020	39.668	124812921	0.968	61.553	26.261	124812921	0.997
	308	69.951	54.374	171085536	0.997	63.267	33.136	171085536	0.995
	318	73.145	59.432	187002496	0.997	66.140	35.528	187002496	0.994

Table S3. Linear Langmuir isotherm parameters for $H_2PO_4^-/HPO_4^{2-}$ and $HCrO_4^-/CrO_4^{2-}$ ions obtained at 298, 308 and 318 K using WL/MG and WL-γ-APS/MG adsorbents

	$H_2PO_4^-/HPO_4^{2-}$					$HCrO_4^-/CrO_4^{2-}$				
	T **(K)**	q_e **(mg g^{-1})**	***K*** **(l mg^{-1})**	K_L **(l mol^{-1})**	R^2	q_e **(mg g^{-1})**	***K*** **(l mg^{-1})**	K_L **(l mol^{-1})**	R^2
WL/MG	298	45.789	5.073	8721609	0.996	43.993	6.069	17513050	0.999
	308	47.316	5.404	9290532	0.996	45.099	6.542	18878895	0.995
	318	48.643	6.331	10884022	0.981	47.621	6.951	20059692	0.979
WL-γ-APS/MG	298	60.718	6.137	10550703	0.989	62.966	4.660	13447961	0.995
	308	63.094	7.211	12395819	0.989	63.222	7.098	20481959	0.997
	318	64.118	12.90	22175573	0.987	63.346	8.014	23126029	0.996

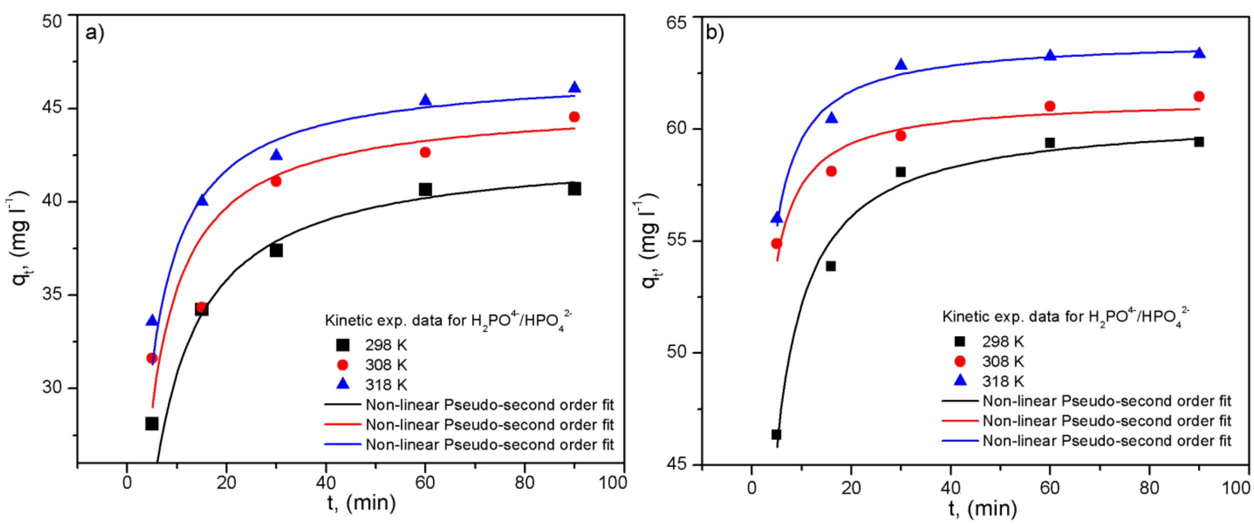

Figure S6. Plot of non-linear pseudo-second-order for $H_2PO_4^-/HPO_4^{2-}$ ions removal by using a) WL-MG and b)WL-γ-APS/MGat 298, 308 and 318K ($C_{i[(H_2PO_4^-/HPO_4^{2-}]}$ = 10 ppm, m/V = 125 mg l^{-1}, pH 6.5 for $H_2PO_4^-/HPO_4^{2-}$)

Table S4. Kinetic parameters obtained by the use of linear PSO kinetic model for the Cd^{2+}, Ni^{2+}, $HCrO_4^-$/CrO_4^{2-} and $H_2PO_4^-$/HPO_4^{2-} removal using WL/MG and WL-γ-APS/MG adsorbents

	298 K		
	Pseudo-second order	Cd^{2+}	Ni^{2+}
WL/MG	k_2x10^2 (g mg^{-1} min^{-1})	0.181±0.031	0.184±0.015
	q_e (mg g^{-1})	56.665±1.045	56.134±1.812
	R^2	0.999	0.998
WL-γ-APS/MG	k_2x10^2 (g mg^{-1} min^{-1})	1.510±0.032	1.478±0.001
	q_e (mg g^{-1})	69.512±1.152	62.020±1.172
	R^2	0.990	0.995
	Pseudo-second order	$H_2PO_4^-$/HPO_4^{2-}	$HCrO_4^-$/CrO_4^{2-}
WL/MG	k_2x10^2 (g mg^{-1} min^{-1})	0.239±0.022	0.233±0.033
	q_e (mg g^{-1})	48.353±1.240	47.531±1.145
	R^2	0.990	0.993
WL-γ-APS/MG	k_2x10^2 (g mg^{-1} min^{-1})	1.044±0.011	0.864±0.019
	q_e (mg g^{-1})	60.546±0.919	61.390±1.198
	R^2	0.997	0.998
	Ea (kJ mol^{-1})	22.41	25.35
	308 K		
	Pseudo-second order	Cd^{2+}	Ni^{2+}
WL/MG	k_2x10^2 (g mg^{-1} min^{-1})	0.242±0.022	0.187±0.077
	q_e (mg g^{-1})	58.646±0.837	56.134±0.593
	R^2	0.987	0.998
WL-γ-APS/MG	k_2x10^2 (g mg^{-1} min^{-1})	1.671±0.017	1.645±0.151
	q_e (mg g^{-1})	70.419±1.121	62.930±0.687
	R^2	0.999	0.998
	Pseudo-second order	$H_2PO_4^-$/HPO_4^{2-}	$HCrO_4^-$/CrO_4^{2-}
WL/MG	k_2x10^2 (g mg^{-1} min^{-1})	0.377±0.015	0.261±0.028
	q_e (mg g^{-1})	48.933±1.024	48.366±1.268
	R^2	0.995	0.994
WL-γ-APS/MG	k_2x10^2 (g mg^{-1} min^{-1})	1.217±0.025	1.113±0.058
	q_e (mg g^{-1})	62.818±0.968	63.307±1.205
	R^2	0.999	0.998
	318 K		
	Pseudo-second order	Cd^{2+}	Ni^{2+}
WL/MG	k_2x10^2 (g mg^{-1} min^{-1})	0.308±0.027	0.233±0.010
	q_e (mg g^{-1})	59.145±1.066	59.420±1.078
	R^2	0.9997	0.996
WL-γ-APS/MG	k_2x10^2 (g mg^{-1} min^{-1})	2.104±0.002	2.109±0.001
	q_e (mg g^{-1})	73.560±1.057	66.157±1.102
	R^2	0.999	0.999
	Pseudo-second order	$H_2PO_4^-$/HPO_4^{2-}	$HCrO_4^-$/CrO_4^{2-}
WL/MG	k_2x10^2 (g mg^{-1} min^{-1})	0.404±0.028	0.447±0.013
	q_e (mg g^{-1})	50.474±1.201	48.996±0.987
	R^2	0.996	0.999
WL-γ-APS/MG	k_2x10^2 (g mg^{-1} min^{-1})	1.848±0.087	1.576±0.013
	q_e (mg g^{-1})	63.9997±1.021	63.654±0.987
	R^2	0.999	0.999

Adsorption kinetic study

General uptake mechanism, analyzed according to pseudo-second-order equation, consider one rate controlling step and did not offer valuable information on adsorption mechanism. Therefore, the intra-particle diffusion model *i.e.* Weber-Morris model, was applied to analyze mass transfer phenomena of overall process. Kinetic model consider four consecutive steps: adsorbate transport in the bulk, diffusion through the liquid film surrounding the surface of the particle (external mass transfer or film diffusion), diffusion through the pores inside of particles (intra-particle diffusion) and last step is a chemical reaction (adsorption/desorption) of adsorbate with active sites present at surface matrix, *i.e.* mass action.

Table S5. Kinetic parameters obtained by the use of interparticle diffusion Weber-Morris model for the Cd^{2+}, Ni^{2+}, $HCrO_4^-/CrO_4^{2-}$ and $H_2PO_4^-/HPO_4^{2-}$ removal using WL/MG and WL-γ-APS/MG adsorbents

298 K			
	Weber-Morris	Cd^{2+}	Ni^{2+}
WL/MG	k_{p1} (mg g^{-1} min$^{-0.5}$)	4.767±0.112	4.769±0.012
	C_1 (mg g^{-1})	13.959±0.982	14.202±0.915
	k_{p2} (mg g^{-1} min$^{-0.5}$)	0.015±0.002	0.062±0.001
	C_2 (mg g^{-1})	50.588±1.002	47.770±1.151
	R^2	0.999	0.984
WL-γ-APS/MG	k_{p1} (mg g^{-1} min$^{-0.5}$)	5.196±0.210	5.196±0.021
	C_1 (mg g^{-1})	44.992±0.887	37.492±1.025
	k_{p2} (mg g^{-1} min$^{-0.5}$)	0.176±0.004	0.175±0.001
	C_2 (mg g^{-1})	67.073±0.960	59.566±0.998
	R^2	0.903	0.934
	Weber-Morris	$H_2PO_4^-/HPO_4^{2-}$	$HCrO_4^-/CrO_4^{2-}$
WL/MG	k_{p1} (mg g^{-1} min$^{-0.5}$)	0.944±0.011	2.529±0.102
	C_1 (mg g^{-1})	26.062±1.140	15.299±1.028
	k_{p2} (mg g^{-1} min$^{-0.5}$)	0.0862±0.001	0.939±0.024
	C_2 (mg g^{-1})	43.657±1.215	34.580±1.020
	R^2	0.999	0.874
WL-γ-APS/MG	k_{p1} (mg g^{-1} min$^{-0.5}$)	3.999±0.109	4.034±0.112
	C_1 (mg g^{-1})	37.426±0.982	38.254±1.117
	k_{p2} (mg g^{-1} min$^{-0.5}$)	0.203±0.005	0.849±0.0125
	C_2 (mg g^{-1})	57.636±1.057	52.561±0.012
	R^2	0.897	0.998

Table S6. Comparison of adsorbents WL and magnetite based adsorbent for heavy metal and oxyions adsorption

Adsorbent	Ion	C_i, mg l^{-1}	q_e, mg g^{-1}	reference
Wollastonite	Ni^{2+}	50.0	6.50	(Sharma et al. 1990)
Wollastonite	$HCrO_4^-/CrO_4^{2-}$	5.0	21.92	(Obradović et al. 2017)
Wollastonite	phosphate ions	5.0	27.29	(Obradović et al. 2017)
QFW*	Cr^{6+}	10.0	9.81	(Petrova et al. 2011)
Magnetite nanoparticles	Cr^{6+}	80.0	13.5 (pH 2.5)	(Martínez et al. 2015)
MG nanospheres	Cr^{6+}	10.0	8.90 (45°C)	(Kumari et al. 2015)
Sulfate-modified MG nanoparticles	Cd^{2+}	-	7.90	(Babaei et al. 2014)
Synthetic mineral adsorbent**	Cd^{2+}	-	47.0	(Chen et al. 2017)
W-MG	Ni^{2+}	10.0	52.41	This work
W-MG	Cd^{2+}	10.0	55.75	This work
W-MG	$HCrO_4^-/CrO_4^{2-}$	10.0	47.62	This work
W-MG	$H_2PO_4^-/HPO_4^{2-}$	10.0	48.64	This work
WL-γ-APS/MG	Ni^{2+}	10.0	66.14	This work
WL-γ-APS/MG	Cd^{2+}	10.0	73.15	This work
WL-γ-APS/MG	$HCrO_4^-/CrO_4^{2-}$	10.0	63.35	This work
WL-γ-APS/MG	$H_2PO_4^-/HPO_4^{2-}$	10.0	64.12	This work

*QFW-quartz/feldspar/wollastonite; ** Synthetic mineral adsorbent containing wollastonite, illite, gypsum, limestone and dolomite

References

Babaei AA, Bahrami M, Farrokhian Firouzi A, et al (2014) Adsorption of cadmium onto modified nanosized magnetite: kinetic modeling, isotherm studies, and process optimization. Desalin Water Treat 1–13. doi: 10.1080/19443994.2014.972986

Chen G, Shah KJ, Shi L, Chiang P-C (2017) Removal of Cd(II) and Pb(II) ions from aqueous solutions by synthetic mineral adsorbent: Performance and mechanisms. Appl Surf Sci 409:296–305. doi: 10.1016/j.apsusc.2017.03.022

Kumari M, Pittman CU, Mohan D (2015) Heavy metals [chromium (VI) and lead (II)] removal from water using mesoporous magnetite (Fe_3O_4) nanospheres. J Colloid Interface Sci 442:120–132. doi: 10.1016/j.jcis.2014.09.012

Martínez LJ, Muñoz-Bonilla A, Mazario E, et al (2015) Adsorption of chromium(VI) onto electrochemically obtained magnetite nanoparticles. Int J Environ Sci Technol 12:4017–4024. doi: 10.1007/s13762-015-0832-z

Obradović N, Filipović S, Marković S, et al (2017) Influence of different pore-forming agents on wollastonite microstructures and adsorption capacities. Ceram Int 43:7461–7468. doi: 10.1016/j.ceramint.2017.03.021

Petrova TM, Fachikov L, Hristov J (2011) the magnetite as adsorbent for some hazardous species from aqueous solution: A review. Int Rev Chem Eng Int Rev Chem Eng 3:134–152

Sharma YC, Gupta GS, Prasad G, Rupainwar DC (1990) Use of wollastonite in the removal of Ni(II) from aqueous solutions. Water Air Soil Pollut 49:69–79. doi: 10.1007/BF00279511